J Fusion Energ (2016) 35:148–153
DOI 10.1007/s10894-015-9974-8

ORIGINAL RESEARCH

Code Validation for Magnetohydrodynamic Buoyant Flow at High Hartmann Number

Zi Meng[1,2] · Muyi Ni[1] · Jieqiong Jiang[1] · Zhiqiang Zhu[1] · Tao Zhou[1]

Published online: 30 July 2015

Abstract In liquid metal fusion blanket, the non-uniform volumetric heat deposited by the fusion neutrons leads to the non-uniform density distribution of liquid metal. With the force of gravity, buoyant flows would happen. In the fusion blanket where the magnetic field is up to 4T or even higher and the Hartmann number is $\sim 10^4$, these effects caused by the buoyancy will significantly influence the flow and heat transfer characteristics. In this paper, a module for magnetohydrodynamic (MHD) buoyant flow at high Hartmann number was added to the code MTC. A current density conservative scheme was used to ensure the conservation of current, and the Boussinesq model was used to simulate the buoyancy force. This code was validated by two benchmarks, and the results showed that it can give an accurate simulation for MHD buoyant flows. Main characteristics of buoyancy effects of MHD flows were investigated, and the suppression of buoyant convection by strong magnetic field was studied to understand how the direction of magnetic field and electric conductivity of wall affects the suppression.

Keywords High Hartmann number · MHD · Buoyant flow

✉ Tao Zhou
tao.zhou@fds.org.cn

[1] Key Laboratory of Neutronics and Radiation Safety, Institute of Nuclear Energy Safety Technology, Chinese Academy of Sciences, No. 350 Shushanhu Road, Hefei 230031, Anhui, China

[2] University of Science and Technology of China, Hefei 230026, Anhui, China

Introduction

Fusion energy [1–3] is a potential choice of human energy for its sustainable energy source, low risk of severe accidents, short-lived radioactive waste. Also Fusion reactor is a good choice for nuclear waste transmutation [4, 5] and hydrogen production [6]. Blanket is a key component for energy transformation and extraction in fusion reactor [7], and the liquid metal breeder blanket concept [8–10] has been studied extensively in the world due to their high heat removal, adequate tritium breeding ratio, relative simple design, potential attractiveness of economy and safety [11–15]. However for magnetically confined fusion reactors, the strong magnetic field used for confinement of the fusion plasma will have impacts on velocity distribution, heat transfer characteristics, pressure drop and the required pumping power for the cooling system. The use of liquid metal in the liquid blankets of fusion devices will lead to MHD effects, which are among the most important considerations in any liquid metal blanket concept [16].

For fusion blanket, the volumetric nuclear heat deposited in blankets has a steep gradient, which makes the liquid metal in blanket volume experience different expansion and form non-uniform density distribution. With the force of gravity, the non-uniform density forms buoyant flow in liquid blanket [17]. In ITER and future DEMO plants, the Grashof number, which stands for the ratio of buoyancy force to viscous force, would reach $10^7 \sim 10^{12}$ [17, 18]. In the cases the buoyant flow would be comparable to or even surpass the forced flow, and forms natural convection or mixed convection. In liquid metal blanket under strong magnetic field, the natural convection and mixed convection are different with common fluid. Its buoyancy characteristic is related not only to Gr, but also to

Ha. The coupled effect of buoyancy and MHD is important to heat transfer and flow of liquid blanket [19–21].

For MHD buoyant flow issues, most researches were based on theory analysis or numerical simulation of simple square duct at small Ha. Bühler [22] developed code IKET based on CFD platform openfoam and investigated buoyant flow in vertical duct under different magnetic fields. Kharicha et al. [18] simulated MHD buoyant flow in HCLL TBM, but the order of Ha was 10^2, which is far smaller than the Ha in liquid blanket ($\sim 10^4$). Smolentsev et al. [17] investigated the mixed convection in DCLL blanket with 2D model and DNS method to simulate turbulence at small Ha. The inability to adequately simulate MHD buoyant flow at large Ha and Gr is due to the complexity of MHD buoyant flow.

In this paper, we developed a buoyant flow module based on code MTC [23, 24], which is a CFD code for MHD analysis. This code adopted the conservative scheme for current and Lorentz force to get numerical conservative current [25]. The buoyancy force was simulated by Boussinesq model. This code was validated by two benchmarks of MHD buoyant flow. One is MHD buoyant flow in a vertical duct, which is a theoretical result [21] and the Hartmann numbers in our simulation reach 2000. The other is MHD natural convection in a cavity [26], which is an experimental result with Hartmann numbers $0 \sim 460$. The simulations matched well with the benchmarks, which show that the code has the ability to accurately simulate MHD buoyant flow under high magnetic fields. Main characteristics of buoyancy effects of MHD flows were investigated, and the suppression of buoyant convection by strong magnetic field was studied to understand how the direction of magnetic field and electric conductivity of wall affects the suppression.

Methods and Models

This buoyant flow module was developed based on code MTC, which is a parallel C ++ code for 3D MHD analysis. The code was composed of three modules: flow field solution, electric potential solution and temperature solution. The flow field solution adopted PISO methods, which is a traditional CFD method fit for transient flow. The electric potential solution was implemented specially with current conservative scheme and was the most important module for MHD flow simulation. The temperature solution was implemented traditionally.

Physical Model of MHD Flow

The physical model of MHD flow in this paper was under several assumptions:

1. The liquid metal flow was incompressible.
2. The density of liquid metal was simulated by Boussinesq model, while other physical properties such as electric conductivity, viscosity, heat conductivity were assumed constant at the temperature range.
3. The magnetic field induced by changing electric field was small relative to the strong external magnetic field.
4. The viscous dissipation and Joulean heating were neglected in the temperature equation.

Under these assumptions, the flow of liquid metal under the influence of strong external magnetic field was governed by the following equations:

Momentum equations:

$$\frac{\partial \vec{u}}{\partial t} + \vec{u} \cdot \nabla \vec{u} = -\nabla p + \frac{1}{\mathrm{Re}} \nabla^2 \vec{u} + N(\vec{J} \times \vec{B}) + \vec{f} \tag{1}$$

Continuity equation:

$$\nabla \cdot \vec{u} = 0 \tag{2}$$

Temperature equation:

$$\frac{\partial T}{\partial t} + \vec{u} \cdot \nabla T = \frac{1}{Pe} \nabla^2 T + Q \tag{3}$$

Ohm's law:

$$\vec{J} = -\nabla \varphi + \vec{u} \times \vec{B} \tag{4}$$

And the current density was conservative, such that

$$\Delta \varphi = \nabla \cdot \left(\vec{u} \times \vec{B} \right) \tag{5}$$

In above equations, $\vec{u}$, p, T were the non-dimensional velocity vector, pressure and temperature scaled with characteristic velocity $u_0, \rho u_0^2, \Delta T$ respectively. Let L be characteristic length, η be fluid kinematic viscosity and σ be fluid conductivity, then $\mathrm{Re} = u_0 L/\eta$ was the Reynolds number, $\mathrm{Ha} = LB_0\sqrt{\sigma/\rho\eta}$ was the Hartmann number which stands for ratio of Lorentz force to viscosity force, $\mathrm{Pe} = \rho c_p u_0 L/\lambda$ was the Peclet number which stands for ratio of convective heat transfer to diffusive heat transfer. The force $\vec{f}$ in Eq. (1) is the buoyancy force. According to Boussinesq model $(\rho_\infty - \rho) \approx \rho\beta(T - T_\infty)$, we get $\vec{f} = \vec{g}\beta(T - T_\infty)$.

Solution Methods

The process of MHD simulation includes flow field solution, electric potential solution and temperature solution. The solution of temperature field is common and is not introduced here. The flow field was calculated with the PISO (pressure implicit split operator) algorithm, which is fit for transient compressible flow or incompressible flow. PISO gives true solution of transient process. With this

algorithm, we can get the transient process of MHD flow. The electric potential needs accurate solution since MHD flow is greatly influenced by Lorentz force and sensitive to currents. Here a current conservative scheme was adopted to get conservative currents. The electric potential equation is a Poisson equation. To get a highly conservative current, this Poisson equation needs to be solved more accurate than usual. To improve the solution efficiency, AMG methods were adopted to solve Poisson equation.

Results and Discussion

This code used two MHD buoyant flow benchmarks for validation. Benchmark 1 is theoretical MHD buoyant flow in a vertical duct. Benchmark 2 is experimental MHD natural convection flow in a cavity.

Results Discussion for Benchmark 1

In the first benchmark [21], MHD buoyant flow in vertical ducts was tested. Effects of the direction of temperature gradient with respect to the orientation of magnetic field and the influence of electric conductivity of walls on the flow structure were investigated. The vertical duct is shown as Fig. 1. Two opposite walls were kept at different constant temperature values, so that a heat flux was established between them and other walls were adiabatic. The temperature gradient can be parallel or perpendicular to the imposed magnetic field. Since there were no average flow in this case, so the velocity scale was chosen according to buoyancy force and magnetic field as $u_0 = \rho_0 g \beta \Delta T / B^2 \sigma$.

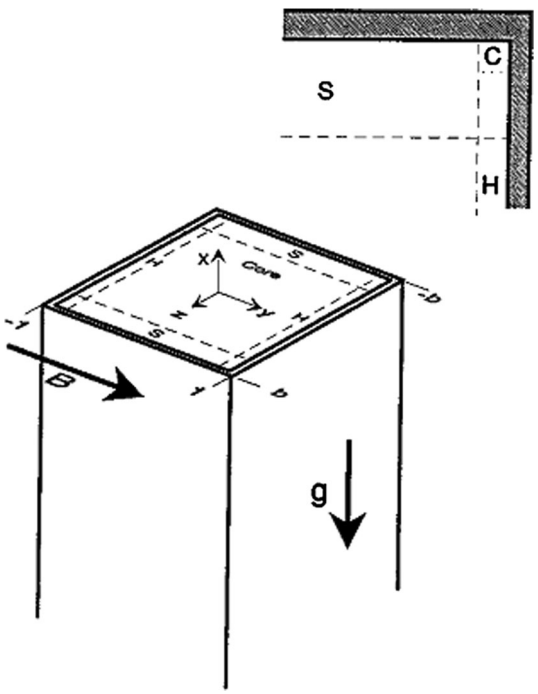

Fig. 1 Structure of vertical duct

In Fig. 2a, MHD buoyant flow with electric conducting wall and $\nabla T \perp B$ was simulated. The simulation result matches well with the theory data. In Fig. 2, we changed the direction and strength of magnetic field and electric conductivity of wall. By comparing the results in Fig. 2, we found the following conclusions:

(1) Magnetic field suppresses buoyant flow: This conclusion is not so clear in Fig. 2 since the velocity is scaled by $u_0 = \rho_0 g \beta \Delta T / B^2 \sigma$. If the original velocity is shown, we would see that, with increasing magnetic field, the velocity would decrease.

(2) High electric conductivity of wall suppresses buoyant flow effectively: By comparing velocity in Fig. 2a, b, we can see that, the velocity in duct with perfectly electric conductive walls is smaller by two orders of magnitude than velocity in duct with electric insulating walls. The reason is that, when the wall is perfectly electric conductive, the current and Lorentz force would be large, which is the direct force suppressing buoyant flow.

(3) The buoyant flow in the case with $\nabla T \parallel B$ is smaller than the case with $\nabla T \perp B$. The reason is related to the current circuit in the duct. When $\nabla T \parallel B$, the current J near the wall is parallel to the wall, where the Lorentz force $\vec{f} = J \times B$ is opposite to the buoyancy force and hinder the buoyant flow. On the other hand, the currents near the opposite wall are in the opposite direction to currents near this wall, which is fit for large current circuit in the duct, as shown in Fig. 3a. When $\nabla T \perp B$, the current J near the wall is perpendicular to the wall. Though the Lorentz force is opposite to the buoyancy force, the currents near the opposite wall are in conflicting direction to currents near this wall, and can't form large current circuit. Instead four small current circuits are formed as shown in Fig. 3b. The current intensity of large current circuit is much stronger than small circuit, so the suppression is larger.

Results Discussion for Benchmark 2

The second benchmark by Okada [26] is natural convection of molten gallium suppressed under an external magnetic field as shown in Fig. 4. In this experiment, the heat transfer rates of natural convection of molten gallium were measured under various strengths of heating rates and directional magnetic fields. Molten gallium was filled in a cubic enclosure of 30 mm × 30 mm × 30 mm where one

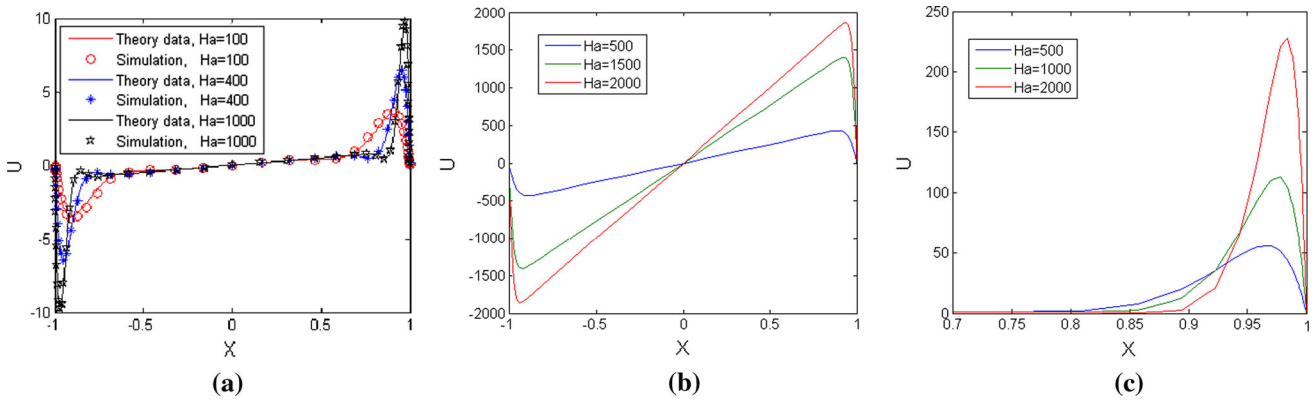

Fig. 2 Buoyancy-driven MHD flow in duct, **a** $\nabla T \perp B$ and electric conducting wall, **b** $\nabla T \perp B$ and electric insulating wall, **c** $\nabla T \parallel B$ and electric insulating wall

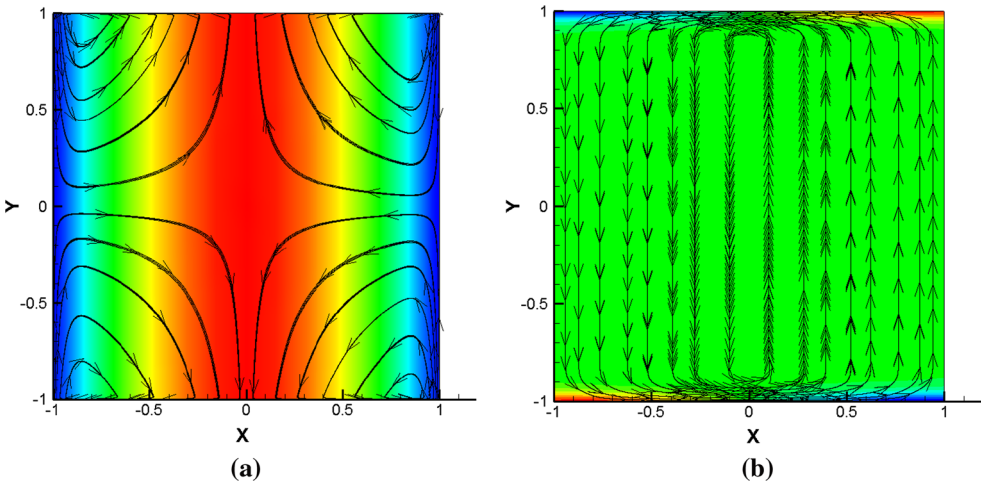

Fig. 3 Electric current streamlines of buoyancy-driven MHD flow in duct, **a** $\nabla T \perp B$, **b** $\nabla T \parallel B$

vertical wall was uniformly heated and an opposing wall was isothermally cooled, with otherwise insulated walls. An external magnetic field was impressed either perpendicular or parallel to the heated wall. For the modified Grashof number $<4.24 \times 10^6$ and the Hartmann number <461, the average Nusslet numbers were measured.

The measured Nusslet numbers were compared with simulation results in Fig. 5. The relative error between them was below 10 %, which proved the validity of the code. Figure 5 shows that with increasing magnetic field, the Nu would decrease, which shows the natural convection is suppressed by this magnetic field. By comparing

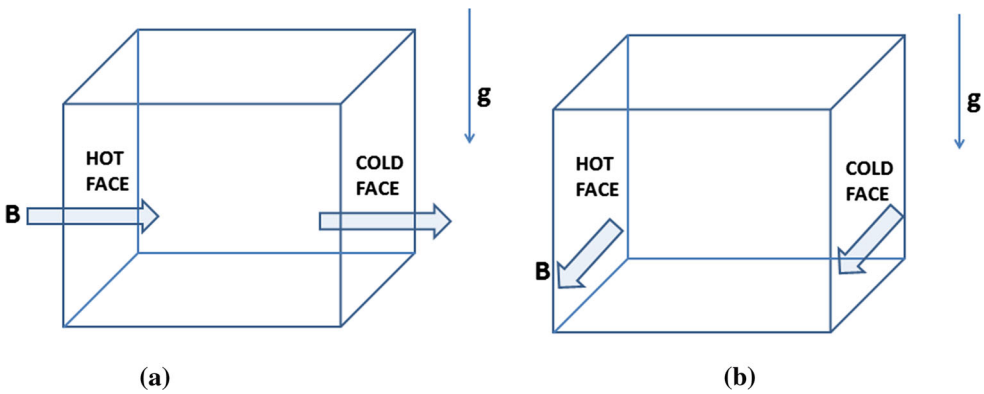

Fig. 4 Natural convection in cavity with **a** $\nabla T \parallel B$, **b** $\nabla T \perp B$

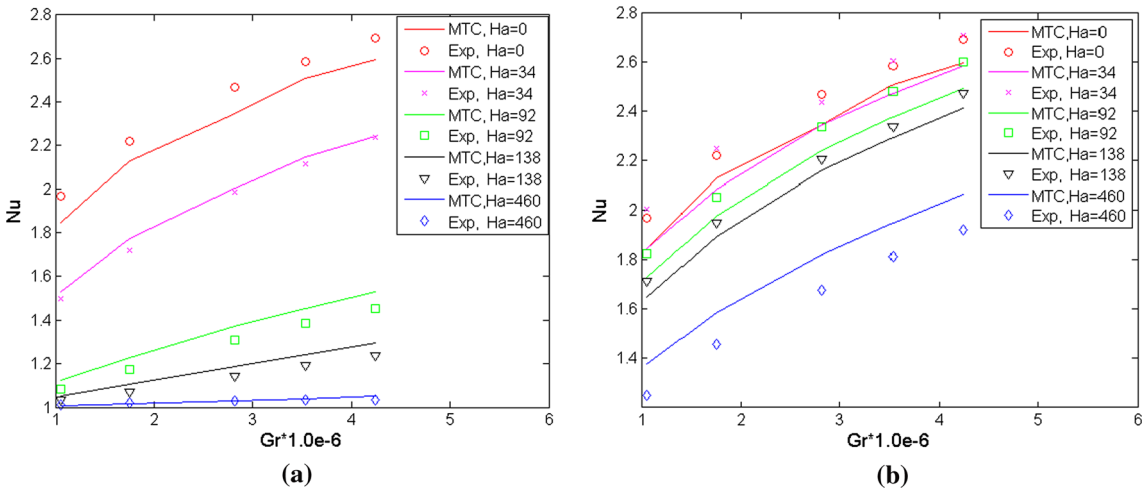

Fig. 5 Nusselt number in natural convection in cavity, simulation data vs. experiment data, **a** $\nabla T \parallel B$, **b** $\nabla T \perp B$

Fig. 5a, b we can see that Nu number with $\nabla T \perp B$ is much larger than the case with $\nabla T \parallel B$, which means that the buoyant flow with $\nabla T \perp B$ is much stronger than the case with $\nabla T \parallel B$. This is in accordance with the phenomenon observed in the benchmark 1.

Summary

To analyze MHD buoyant flow in fusion liquid metal blankets, a buoyant flow simulation module in code MTC was developed. This code was validated by two benchmarks of MHD buoyant flow. The first benchmark was MHD buoyant flow in differentially heated vertical channels, which was a serial of theoretical results with Hartmann numbers $\sim 10^3$. The second benchmark was MHD natural convection flow in a cavity, which was an experimental result with Hartmann numbers $0 \sim 460$. This code gave an accurate simulation of MHD buoyant flow, which demonstrates its ability to accurately simulate MHD buoyant flow under high magnetic fields. Main characteristics of buoyancy effects of MHD flows were investigated, and the suppression of buoyant convection by strong magnetic field was studied to understand how the direction of magnetic field and electric conductivity of wall affects the suppression. In general, the buoyant flow in the case with $\nabla T \parallel B$ was more effectively suppressed than the case with $\nabla T \perp B$, and high electric conductivity of wall suppressed buoyant flow more effectively than walls with low high electric conductivity. This analysis was validated both by the theoretical benchmark and the experimental benchmark, and this understanding of MHD buoyant flow was valuable for improving heat transfer of liquid blanket.

Acknowledgments This work is supported by National Natural Science Foundation of China with Grant No. 11205190, and also by National Magnetic Confinement Fusion Science Program of China under Grant No. 2015GB108005. The authors would like to show their great appreciation to other members of FDS Team for their support and contribution to this work.

References

1. Y. Wu, F.D.S. Team, Conceptual design activities of FDS series fusion power plant in China. Fusion Eng. Des. **81**(23–24), 2713–2718 (2006)
2. Y. Wu, J. Jiang, M. Wang et al., A fusion-driven subcritical system concept based on viable technologies. Nucl. Fusion **51**(10), 103036 (2011)
3. Y. Wu, F.D.S. Team, Conceptual design of the China fusion power plant FDS-II. Fusion Eng. Des. **83**(10–12), 1683–1689 (2008)
4. L. Qiu, Y. Wu, B. Xiao et al., A low aspect ratio tokamak transmutation system. Nucl. Fusion **40**, 629–633 (2000)
5. Y. Wu, J. Qian, J. Yu, The fusion-driven hybrid system and its material selection. J. Nucl. Mater. **307–311**, 1629–1636 (2002)
6. Y. Wu, F.D.S. Team, Fusion-based hydrogen production reactor and its material selection. J. Nucl. Mater. **386–388**, 122–126 (2009)
7. T. IHLI, T.K. Basu, L.M. Giancarli, S. Konishi, S. Malang, F. Najmabadi et al., Review of blanket designs for advanced fusion reactors. Fusion Eng. Des. **83**(7–9), 912–919 (2008)
8. S. Malang, P. Leroy, G.P. Casini, F.F. Mattas, Y. Strebkov, Crucial issues on liquid metal blanket design. Fusion Eng. Des. **16**, 95–109 (1991)
9. Y. Wu, FDS Team, Design status and development strategy of China liquid lithium–lead blankets and related material technology, J. Nucl. Mater. 367–370 (B), 1410–1415 (2007)
10. Y. Wu, F.D.S. Team, Overview of liquid lithium lead breeder blanket program in China. Fusion Eng. Des. **86**, 2343–2346 (2011)
11. Y. Wu, F.D.S. Team, Conceptual design and testing strategy of a dual functional lithium–lead test blanket module in ITER and EAST. Nucl. Fusion **47**(11), 1533–1539 (2007)
12. Q. Huang, C. Li et al., Progress in development of China low activation martensitic steel for fusion application. J. Nucl. Mater. **367–370**, 142–146 (2007)
13. G. Rampal, A.L. Puma, Y. Poitevin, E. Rigal, J. Szczepanski, C. Boudot, HCLL TBM for ITER-design studies. Fusion Eng. Des. **75–79**, 917–922 (2005)

14. C.P.C. Wong, J.F. Salavy, Y. Kim, I. Kirillov, E. Rajendra Kumar, N.B. Morley et al., Overview of liquid metal TBM concepts and programs. Fusion Eng. Des. **83**(7–9), 850–857 (2008)
15. Y. Wu, F.D.S. Team, Design analysis of the China dual-functional lithium lead (DFLL) test blanket module in ITER. Fusion Eng. Des. **82**(2007), 15–24 (1893)
16. S. Smolentsev, R. Moreau et al., MHD thermo-fluid issues of liquid-metal blankets: phenomena and advances. Fusion Eng. Des. **85**, 1196–1205 (2010)
17. S. Smolentsev, T. Moreau, M. Abdou, Characterization of key magnetohydrodynamic phenomena in PbLi flows for the US DCLL blanket. Fusion Eng. Des. **83**(5–6), 771–783 (2008)
18. A. Kharicha, et al., Buoyant convection in the HCLL blanket in a strong, uniform magnetic field, in FZKA 69592004, Forschungszentrum Karlsruhe: Karlsruhe
19. J.-P. Garandet, T. Alboussiere, R. Moreau, Buoyancy driven convection in a rectangular enclosure with a transverse magnetic field. Int. J. Heat Mass Transf. **35**(4), 741–748 (1992)
20. S. Alchaar, P. Vasseur, E. Bilgen, Natural-convection heat-transfer in a rectangular enclosure with a transverse magnetic field. J. Heat Transf. Trans. Asme **117**(3), 668–673 (1995)
21. L. Bühler, Laminar buoyant magnetohydrodynamic flow in vertical rectangular ducts. Phys. Fluids **10**(1), 223–236 (1998)
22. C. Mistrangelo, L. Bühler, Numerical analysis of buoyant-convection liquid metal flow in channels exposed to strong magnetic fields, in *IEEE/NPSS 24th Symposium on Fusion Engineering*, Chicago, IL (2011), pp. 1–6
23. T. Zhou, Z. Meng, H. Zhang et al., Code validation for the magnetohydrodynamic flow at high Hartmann number based on unstructured grid. Fusion Eng. Des. **88**, 2885–2890 (2013)
24. T. Zhou, H. Chen, Z. Yang, Effect of fringing magnetic field on magnetohydrodynamic flow in rectangular duct. Fusion Eng. Des. **86**, 2352–2357 (2011)
25. M.-J. Ni, J.-F. Li, A consistent and conservative scheme for incompressible MHD flows at a low magnetic Reynolds number, Part III: on a staggered mesh. J. Comput. Phys. **231**(2), 281–298 (2012)
26. K. Okada, H. Ozoe, Experimental heat transfer rates of natural convection of molten gallium suppressed under an external magnetic field in either the X, Y, or Z direction. J. Heat Transf. **114**, 107–114 (1992)